Metallography of Al_5 Mg and Al_{10} Mg alloys modified with 2% Zn after thermal aging treatment

Metalografía de las aleaciones Al_5Mg y $Al_{10}Mg$ modificadas con 2% de Zn después del tratamiento térmico de envejecimiento

Álvaro José Cotes Toro[1], Dino Carmelo Manco-Jaraba[2], Carlos Alberto Socarras Bertiz[3]

[1]Metallurgical Engineer, Master in Management of Research and Development Projects, Specialist in Integrity and Corrosion Management, Universidad de La Guajira. E-mail: ajcotes@uniguajira.edu.co ORCID: https://orcid.org/0000-0003-0402-1565
[2]Mining Engineer, M.Sc. Environmental and Energy Management in Organizations, Universidad de La Guajira. E-mail: dinomancojaraba@gmail.com, ORCID: https://orcid.org/0000-0001-9646-8553
[3]Industrial Engineer, M.Sc. in Process Control and Automation Engineering, Universidad de La Guajira. E-mail: csocarras@uniguajira.edu.co ORCID: https://orcid.org/0000-0002-3801-6943

Cite this article as: A.J. Cotes Toro, D. C. Manco-Jaraba, C. A. Socarras Bertiz "Metallography of Al5Mg and Al10Mg alloys modified with 2% Zn after thermal aging treatment", ", Prospectiva, Vol 23, N° 2, 2025.

Recibido: 12/11/2024 / Aceptado: 16/07/2025

http://doi.org/ 10.15665/rp.v23i2.3698

ABSTRACT

Modern society has the need to obtain materials with better characteristics that help in the use of various applications, so it has always sought new alloys with weight/resistance ratios. In the current work research was carried out on the influence of the addition of a small amount of zinc (2%) on the mechanical properties of two representative aluminum alloys - Magnesium (Al_5 Mg and Al_{10} Mg). The methodology used has several phases, first with a bibliographic study on the principles and fundamentals of heat treatments, subsequently the design of the laundry was carried out by which the specimens are obtained under optimal conditions for the development of this work. Experimental development consists of the selection of the molding medium, model design, fusion and the process of heat treatment of artificial and natural aging of the modified Aluminium-Magnesium alloy, subsequently analysis of the influence of cooling speed, metallographic analysis and grain size. Concluding the coking at high cooling speeds and the poor colability of the alloy results in a very rapid solidification of the specimen, having the characteristic of a fine grain size and absence of macroscopic porosities, as well as a clean and bright surface finish; the temperature and time of heat treatment had a great influence on the variation in grain size due to the solute concentration of each specimen.

Keywords: aluminum-magnesium alloys, aging, heat treatments, metallography.

SUMMARY

La sociedad moderna cuenta con la necesidad de obtener materiales con mejores características que ayuden en la utilización de diversas aplicaciones, por lo que ha buscado siempre nuevas aleaciones con relaciones peso/resistencia. En el actual trabajo se realizó una investigación sobre la influencia de la adición de una pequeña cantidad de zinc (2%) sobre las propiedades mecánicas de dos aleaciones representativas de Aluminio – Magnesio (Al_5Mg y $Al_{10}Mg$). La metodología empleada cuenta con varias fases, primero con un estudio bibliográfico sobre los principios y fundamentos de tratamientos térmicos, posteriormente se realizó el diseño de la colada mediante el cual se obtienen las probetas en condiciones óptimas para el desarrollo de este trabajo. El desarrollo experimental consta de la selección del medio de moldeo, diseño de modelos, fusión y el proceso de tratamiento térmico de envejecimiento artificial y natural de la aleación Aluminio- Magnesio modificada, posteriormente se efectuaron análisis de la influencia de la velocidad de enfriamiento, análisis metalográfico y de tamaño de grano. Concluyendo la coquinación a elevadas velocidades de enfriamiento y la pobre colabilidad propia de la aleación da como resultado una solidificación muy rápida de la probeta, teniendo la característica de un fino tamaño de grano y ausencia de porosidades macroscópica, así como un acabado superficial limpio y brillante; la temperatura y el tiempo del tratamiento térmico tuvieron mucha influencia en la variación del tamaño de grano debido a la concentración de solutos de cada probeta.

Keywords: aleaciones de aluminio-magnesio, envejecimiento, metalografía, tratamientos térmicos.

1. INTRODUCTION

In modern industry one of the main materials used is aluminum due to its characteristics to be combined and its properties for various applications, due to its low density, corrosion resistance, electrical conductivity and relatively low price in the market. [1]-[5]. Despite this, it has only been known as a metal for approximately 180 years, being a relatively young metal on the world industrial scene compared to other metals such as iron, which has been influencing our lives for more than two thousand years [6], [7].

Technological advances seek materials with much better characteristics, for them it is necessary to alloy metals with other elements, mainly copper, magnesium, manganese, silicon and zinc, which influence in one way or another on the mechanical strength as well as on the other properties of aluminum. [8]-[10]. The choice of Al5Mg and Al10Mg alloys modified with 2% Zn responds to their technological relevance within the family of non-heat treatable alloys of the 5XXX group, widely used in the naval, aerospace, automotive and transportation industries, due to their excellent corrosion resistance, good weldability and adequate weight/mechanical strength ratio, where they are used for structural parts, and in the automotive industry in rims and decorative parts [11]–[17]. The controlled addition of zinc in moderate proportions has the potential to improve mechanical properties through solid solution hardening and aging mechanisms, without significantly compromising ductility or corrosion resistance.

This work aims to show the influence of the cooling rate, metallographic analysis and grain size of two representative alloys of the 5XXX group, Al_5 Mg and Al_{10} Mg. Seeking to offer, in complement with future research, a scientific contribution, hoping to open a new horizon of research and development, which will provide perspectives and new fields of application for these alloys, always hand in hand with the need for new materials with special characteristics for specific applications.

2. METHODS

This research develops an experimental methodology aimed at the microstructural analysis of Al5Mg and Al10Mg alloys modified with 2% Zn. First, a literature review was conducted on the principles and fundamentals of heat treatment, followed by the design of the casting, obtaining specimens in optimal conditions based on data found in the Foseco casting guide [18]. For this study, four alloys were produced: A1 (Al_3Mg) in As Cast state, sand cast; A2 (Al_3Mg_3Zn) in Sand Cast state; and B1 (Al_3Mg) in As Cast state, cast from commercial aluminum with a purity of 99.7%, using a temperature-controlled electric crucible furnace. The magnesium and zinc were incorporated in a liquid state, under controlled stirring and flux-protected conditions, to ensure adequate homogenization of the alloying elements. The molten alloys were subsequently poured into two types of molds: green sand and preheated metallic, to study the effect of cooling rate on the microstructure. The resulting samples were subjected to heat aging at temperatures of 150°C and 200°C for different exposure times, to analyze their influence on grain size and metallographic characteristics.

Microstructural characterization was carried out using optical metallographic techniques, following procedures standardized under ASTM E3-11 and ASTM E112 [19], [20]. The sample surfaces were prepared by grinding, polishing, and chemical etching with reagents specific for aluminum alloys. The metallographic analysis included grain size measurement using the line intersection method (Jeffries), as well as the identification of phases and morphologies present in the metal matrix. Additionally, differences in microstructure between the heat-treated and molten samples were documented, with emphasis on the formation of dendritic structures, the presence of porosity, and phase distribution. All collected data were analyzed comparatively to establish correlations between process variables (composition, cooling rate, and heat treatment) and the observed metallographic response. This study aimed to analyze the metallography of Al5Mg and Al10Mg alloys modified with 2% Zn after aging heat treatment.

3. RESULTS AND DISCUSSIONS

3.1 influence of cooling rate

To observe the influence of the cooling speed on the part to be obtained, a metal mold was used, it was preheated to 180ºC using a gas torch for 20 minutes before casting, the temperature at the time of casting was 140ºC, the temperature of the molten alloy at the time of casting was recorded in the range of 700ºC to 720ºC, the casting times were recorded in the range of 8.5 to 10 seconds.

When casting in a die, the high cooling rate and the poor castability of the alloy result in a very rapid solidification of the specimen, as a consequence of which the molten metal does not completely fill the mold even under the best conditions of temperature and casting times. In addition, there is the presence of strong internal shrinkage in the critical joining areas. Positive aspects are: a fine grain size and practically no macroscopic porosity, as well as a clean and bright surface finish (Figure 1).

With respect to the sand castings, the presence of black spots was observed on the upper surface of the cast specimens, this effect is more marked in the Al alloy$_{10}$ Mg, due to the increase of magnesium and the prolonged time that the piece needs for its total solidification and consequently there is more time for the hydrogen to diffuse in the alloy.

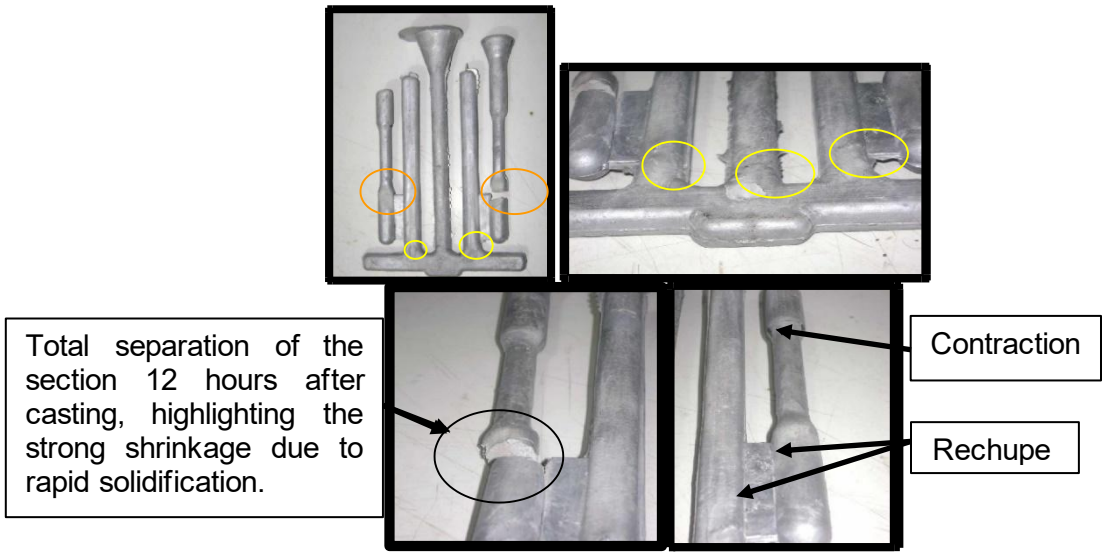

Figure 1. A: Casting in metal shell; B: Detail of critical points, junction zone, upward flow of metal; C: Breakage in the junction section, fillet at 90º; D: Detail shrinkage and shrinkage in the specimen.

This metal/mold reaction results from the action of the magnesium present in the splitting of the moisture present in the sand into its constituents, hydrogen and oxygen. The latter forms the oxide with the alloy and the hydrogen ($Mg + H\ O_2 \rightarrow 2H + MgO$), in atomic state, is dissolved in the liquid metal. When the piece solidifies the hydrogen is expelled from the metal, and the amount that does not reach the atmosphere is retained inside the piece forming the characteristic porosity, concentrated in the parts close to the surface and decreasing towards the center of the piece. Even when the molds are made in sand bonded with sodium silicate and dried before pouring the liquid metal, there is enough water in the atmosphere and on the surface of the mold to react with the magnesium [21], [22].

3.2 Metallographic analysis

The metallographic characterization of the phases present was performed under the optical microscope by identifying the phases and precipitates present using selective etching [11]-[17].

The experimental matrix developed in this study (Table 1) establishes a factorial design that allows a comparative evaluation of the influence of heat aging treatment on two Al-Mg-Zn alloys, with magnesium contents of 5% and 10%, and a constant addition of 2% zinc. Conditions T1 and T2 correspond to treatments carried out at 150°C and 200°C, respectively, with aging times of 10, 12, 14 and 16 hours for each alloy. This design seeks to identify the interaction between Mg content, temperature and treatment time on microstructural evolution, particularly in terms of grain size, secondary phase morphology and precipitation hardening potential. By keeping the Zn concentration constant and varying the thermal conditions and the amount of Mg, it is possible to isolate the individual and combined effects of these variables, allowing the analysis of the precipitation pathways specific to these alloys. Additionally, the study included a detailed characterization of the metallographic phases (Table 2) through the application of six different reagents (1m to 6m), revealing distinct behaviors under chemical attack. It was observed, for example, that reagent 4m is effective in delineating the grain boundaries of the α-Al phase, while the To2 Faith phase showed high reactivity when stained black by reagents 2m to 5m. The Mg_2Si phase showed a variable response, from complete dissolution with reagent 1m to resistance to attack with 3m and 5m, suggesting sensitivity to the chemical composition of the developer. The intermetallic phases $AlMn_6$ and $Al_6(MnFe)$ showed greater stability, with mild attacks or color changes that facilitated their identification, and the $Al_{18}CrMg_{23}$ phase

was selectively attacked by reagents 1m and 2m. These results are essential for the selection of appropriate reagents for the metallographic characterization of complex alloys, as they allow for optimizing the contrast between phases and improving the accuracy of interpreting their structural evolution in response to heat treatment.

Table 1. Nomenclature used.

Group	*Composition*	*Identification*	*Condition*
T1 (150ºC)	Al Mg Zn_{52}	T1 - A10	Al Mg_{52} Zn, aged at 150ºC x 10 Hours
		T1 - A12	Al Mg_{52} Zn, aged at 150ºC x 12 Hours
		T1 - A14	Al Mg_{52} Zn, aged at 150ºC x 14 Hours
		T1 - A16	Al Mg_{52} Zn, aged at 150ºC x 16 Hours
	Al Mg Zn_{102}	T1 - B10	Al Mg_{102} Zn, aged at 150ºC x 10 Hours
		T1 - B12	Al Mg_{102} Zn, aged at 150ºC x 12 Hours
		T1 - B14	Al Mg_{102} Zn, aged at 150ºC x 14 Hours
		T1 - B16	Al Mg_{102} Zn, aged at 150ºC x 16 Hours
T2 (200ºC)	Al Mg Zn_{52}	T2 - A10	Al Mg_{52} Zn, aged at 200ºC x 10 Hours
		T2 - A12	Al Mg_{52} Zn, aged at 200ºC x 12 Hours
		T2 - A14	Al Mg_{52} Zn, aged at 200ºC x 14 Hours
		T2 - A16	Al Mg_{52} Zn, aged at 200ºC x 16 Hours
	Al Mg Zn_{102}	T2 - B10	Al Mg_{102} Zn, aged at 200ºC x 10 Hours
		T2 - B12	Al Mg_{102} Zn, aged at 200ºC x 12 Hours
		T2 - B14	Al Mg_{102} Zn, aged at 200ºC x 14 Hours
		T2 - B16	Al Mg_{102} Zn, aged at 200ºC x 16 Hours

Table 2. Identification of selective attack. Phases by procedure.

Phase	*Reagents and effects*					
	1m	*2m*	*3m*	*4m*	*5m*	*6m*
Yes		Not attacked			Delineate	
α-Al					Reveals grain boundaries	
To_2 Faith		Black	Black	Black	Black	
Mg_2 Si	Dissolves it	Oscurese	Does not attack	Brown	Blue/Not attacked	Darken
Al Mn_6	Not attacked	Not attacked	Bright blue	Brown	Mild attack	Not attacked
Al_6 (MnFe)		Not attacked	Mild attack	Black	Dark gray	Black
Al_{18} Cr Mg_{23}	Attack	Attack	Not attacked	Not attacked	Not attacked	Not attacked

Figure 2 shows the microstructure of a thermally aged Al-Mg-Zn alloy sample, in which intermetallic phases with elongated dendritic morphology are identified, distributed throughout the matrix. These structures, stained blue and gray by the action of the metallographic reagent, are attributable to compounds such as Mg_2Si, $Al_6(MnFe)$, or $Al_{18}CrMg_{23}$, whose response to chemical attack coincides with previously established patterns. Additionally, multiple small spherical porosities are evident, indicated by circles, probably associated with gas entrapment or contraction voids during the solidification stage. The coexistence of these phases with pores reveals a heterogeneous microstructure, influenced by both the cooling rate and the dynamics of the applied heat treatment. The presence of these discontinuities could compromise the material's mechanical properties, particularly its fatigue resistance, underscoring the importance of rigorous control of casting and aging parameters to ensure optimal structural integrity in critical applications.

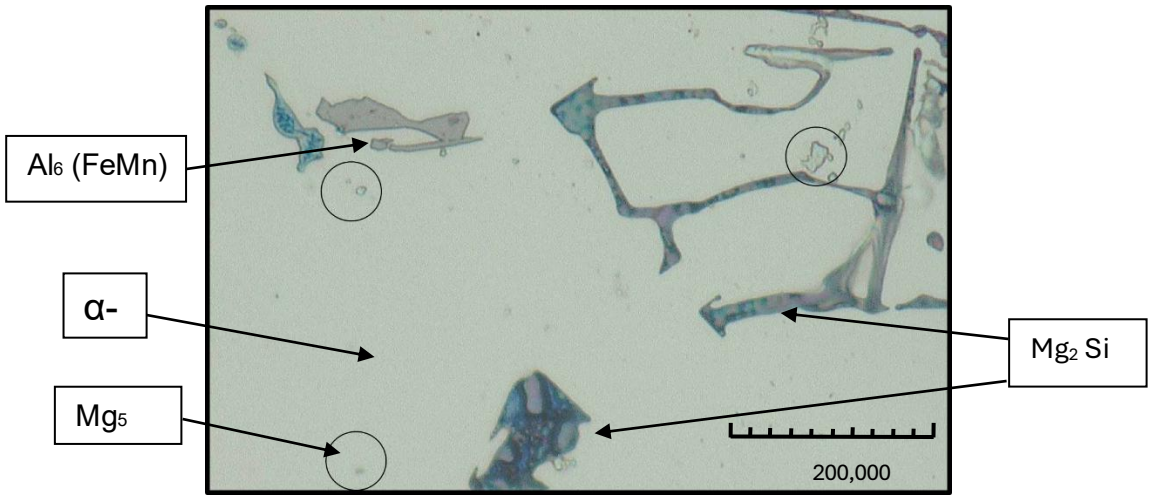

Figure 2. Al_{10} Mg, 3500X without attack. Detail of precipitates.

Las Figuras 3 y 4 presentan el análisis de perfil de línea e imagen tridimensional de la superficie metalográfica de una aleación Al-Mg-Zn envejecida térmicamente. En la Figura 3, el perfil de intensidad obtenido a lo largo de una sección transversal de la microestructura evidencia variaciones significativas en el contraste óptico, correspondientes a cambios abruptos entre la matriz de aluminio y las fases intermetálicas presentes. Estas transiciones, cuantificadas mediante análisis de brillo, reflejan diferencias en la composición química y en la topografía generada tras el ataque químico. Complementariamente, la Figura 4 muestra una reconstrucción tridimensional de la superficie de la muestra, donde se observan zonas de elevación y depresión asociadas a la distinta resistencia de las fases al ataque del reactivo. Los picos de mayor altura corresponden a fases más resistentes (como $Al_6(MnFe)$ o $Al_{18}CrMg_{23}$), mientras que las depresiones indican áreas de mayor disolución, posiblemente ligadas a la fase Mg_2Si. Esta visualización tridimensional refuerza la interpretación microestructural, permitiendo identificar con mayor claridad la distribución, volumen relativo y relieve superficial de las fases presentes, y aporta una herramienta cuantitativa útil para correlacionar las condiciones del tratamiento térmico con la respuesta metalográfica de la aleación.

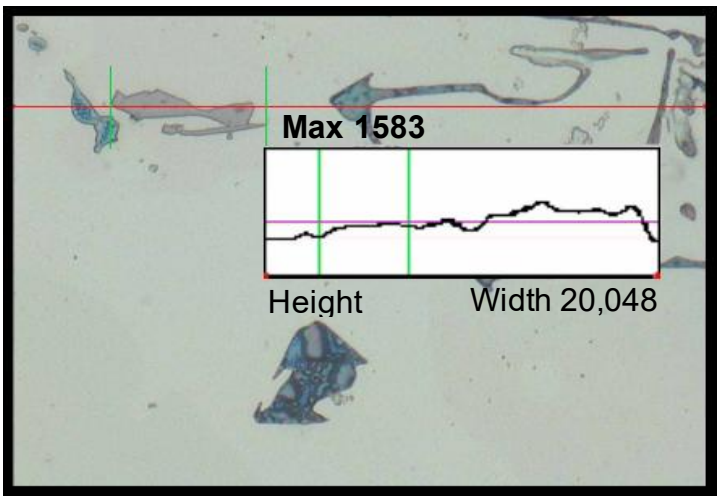

Figure 3. Al_{10} Mg, 3500X without etching. Axial length of the Al_6 (MnFe) precipitate, approximately 1583um.

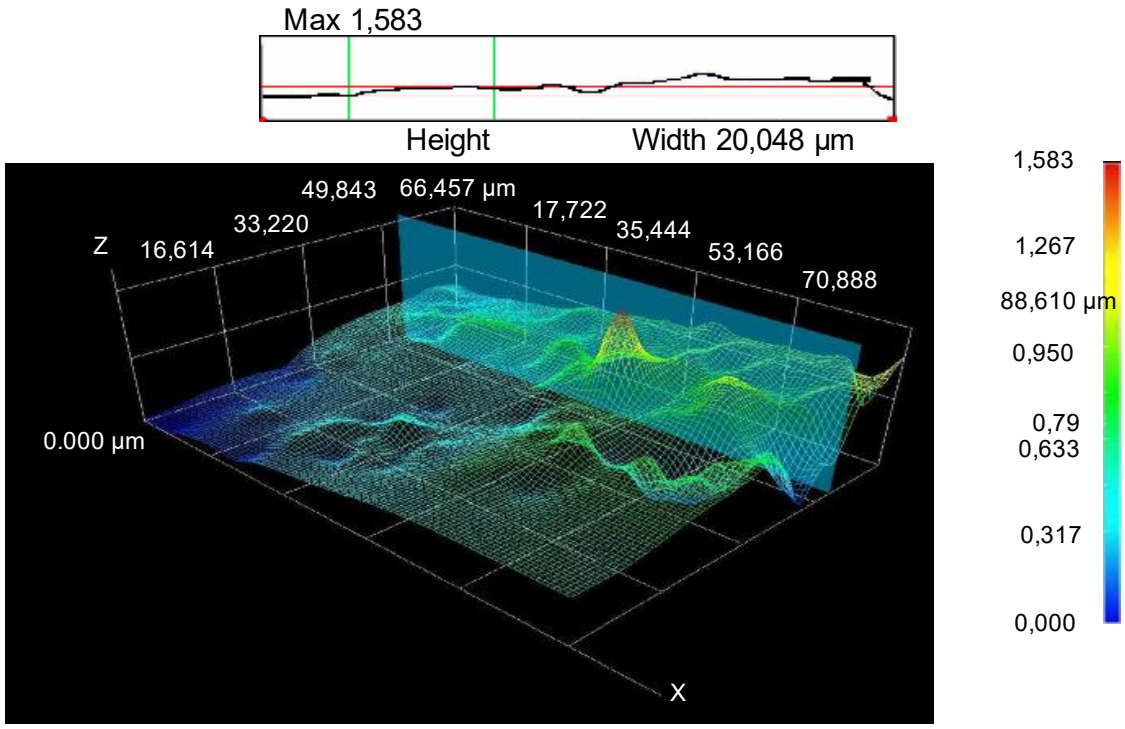

Figure 4. Al_{10} Mg, 3500X without attack. Three-dimensional approach of the Al_6 (MnFe) precipitate.

Metallographs

Figure 4A identifies the phases Mg_2 Si (Chinese letter), the phase Al_6 (FeMn) is found in needle shapes, the eutectic Mg_5 Al8 is not visible; Figure 4B identifies the phases Mg_2 Si (Chinese letter), the phase Al_6 (FeMn) tends to form in a circular shape; the phase Mg_2 Si (Chinese letter) is observed. The Al_6 (FeMn) phase is found to be oval and needle-shaped. The eutectic Mg_5 Al_8 , begins to be seen, as a whitish network, which is confused with the matrix (Figure 4C); Mg_2 Si phases are identified with a tendency to take a more regular shape and to leave the outline of the Chinese letter. The Al_6 (FeMn) phase is resuming the shape of needles. The eutectic Mg_5 Al_8 , is in the form of a much more visible network (Fig. 4D).

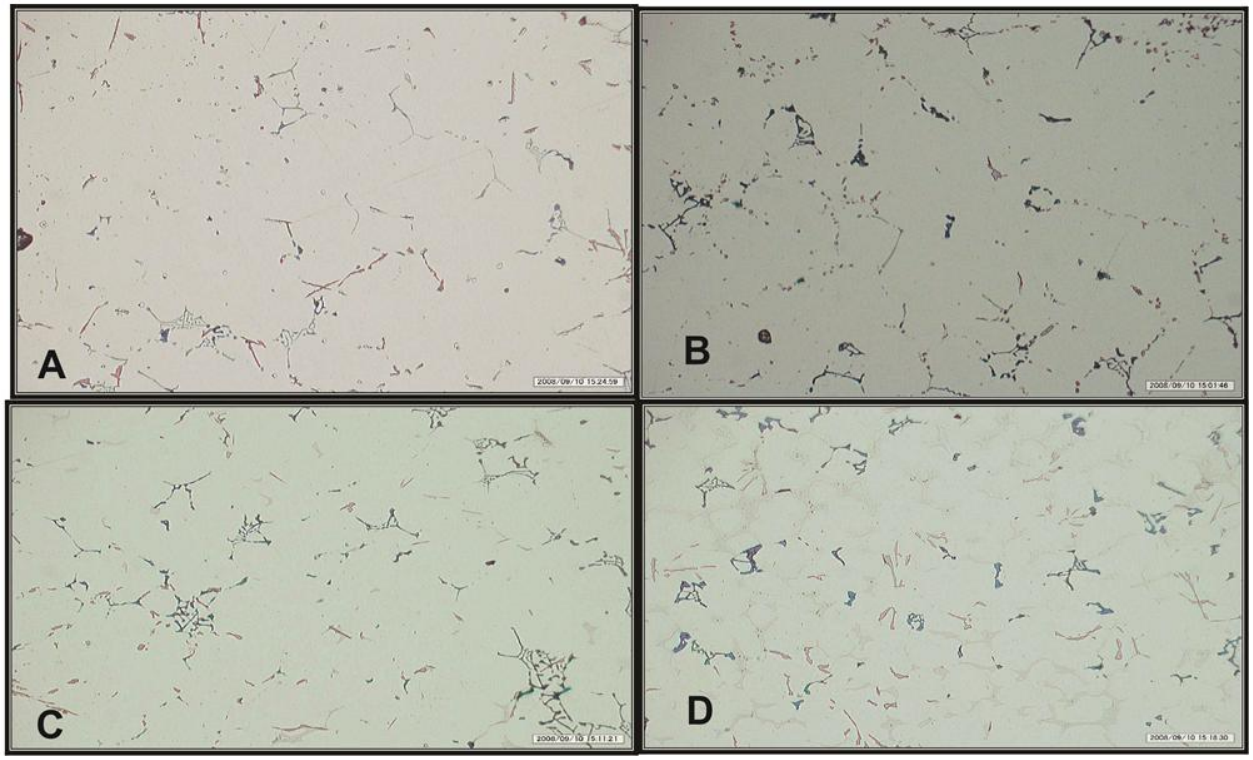

Figure 4. A: Microstructure of the alloy Al_5 Mg 560X without etching; B: Microstructure of the alloy Al_{10} Mg-560X without etching. C: Microstructure of the alloy Al $Mg_{52}Zn$ 560X without etching. D: Microstructure of the alloy Al $Mg_{102}Zn$ 560X without etching.

On Figure 5A it is observed how the eutectic Mg_5Al_8 is formed at the edge of the grain boundaries; the Mg_2 Si phase is observed taking the shape of a Chinese letter, the Al_6(FeMn) phase tends to have curved edges and the eutectic Mg_5 Al_8 is not visible (Figure 5B); Figure 5C shows the Mg_2 Si phase tending to form needles, the Al_6(FeMn) phase tends to have curved edges and the eutectic Mg_5 Al_8 is not visible; Figure 5D shows the Mg_2Si phase and the Al_6(FeMn) phase in less quantity (compared to the previous figure) and the latter in the form of needles, the eutectic Mg_5 Al_8 is not visible.

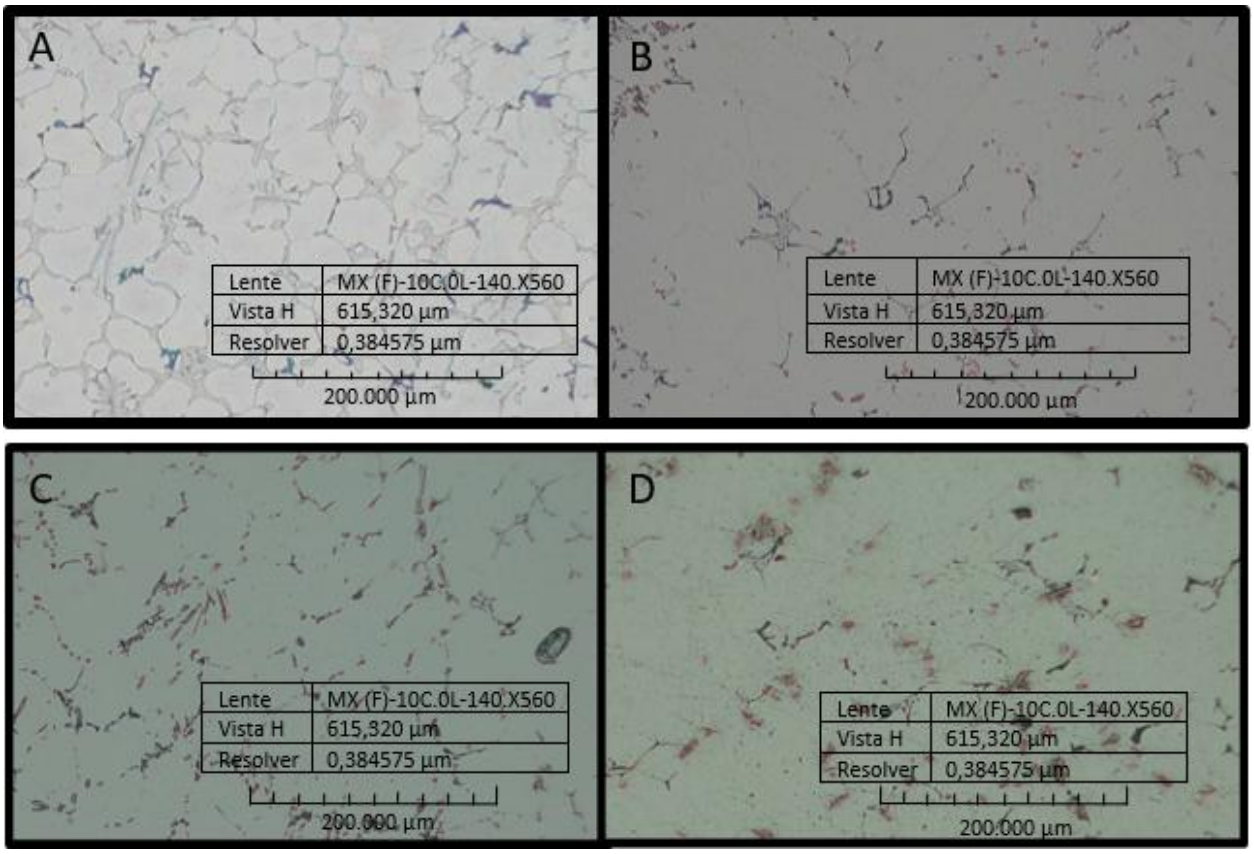

Figure 5. A: Microstructure of alloy Al Mg_{102} Zn 560X attack 4m (NaOH); B: Microstructure of alloy T1-A10 560x without attack; C: Microstructure of alloy T1-A12 560x without attack; D: Microstructure of alloy T1-A14 560x without attack.

Figure 6A and 6B show the Mg_2 Si phase (Chinese letter), the Al_6 (FeMn) phase is found in the form of needles and the eutectic Mg_5 Al_8 , becomes visible (whitish color that blends with the matrix). In Figure 6C the phase Mg_2 Si (Chinese letter) is observed, the phase Al_6 (FeMn) is found with curved edges and the eutectic Mg_5 Al_8 , becomes visible, while in Figure 6D the phase Al_6 (FeMn) is found in oval shape and the eutectic Mg_5 Al_8 is not visible.

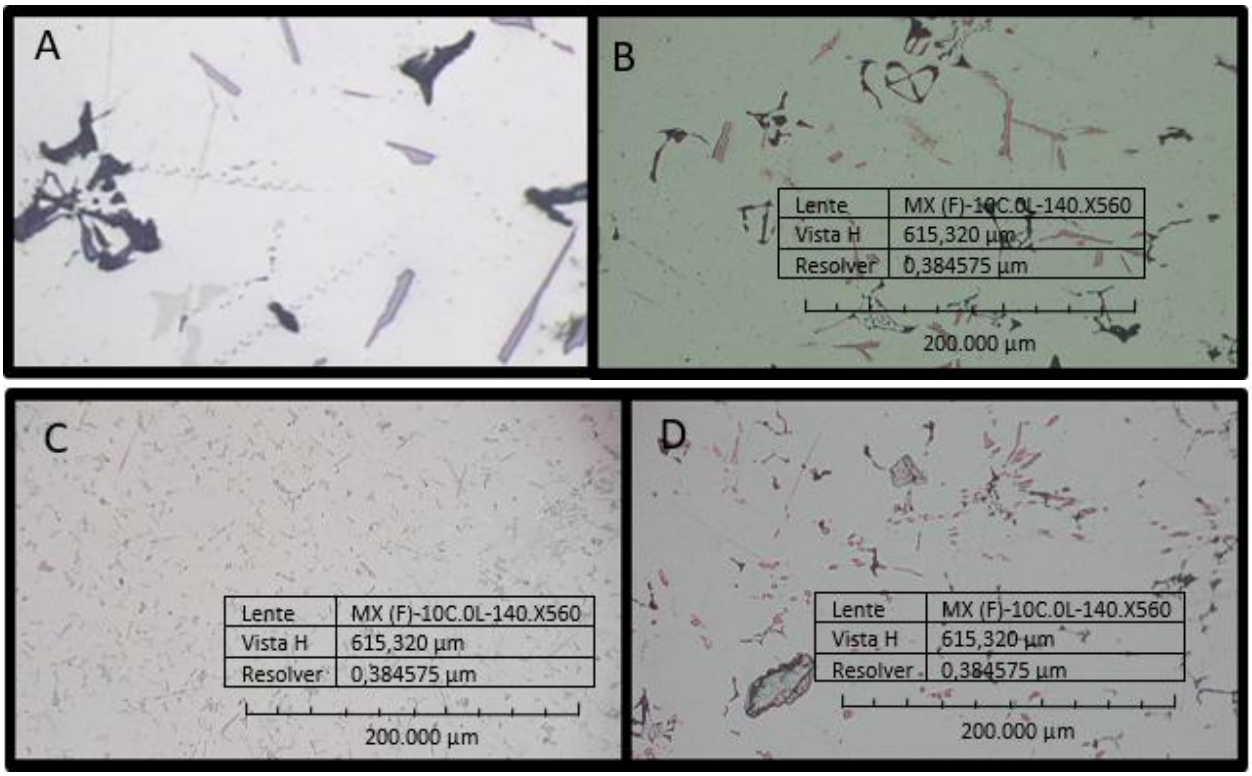

Figure 6. A: Microstructure of alloy T1-A16 560x without etching; B: Microstructure of alloy T1-B10 560x without etching; C: Microstructure of alloy T1-B12 140x without etching; D: Microstructure of alloy T1-B14.560x without etching.

Figure 7A and 7B shows the Mg phase$_2$ Si (Chinese letter) with the Al phase$_6$ (FeMn) in the form of needles. Figure 7C shows the Mg phase$_2$ Si (Chinese letter). The Al$_6$ (FeMn) phase is in less quantity (compared to the previous figure) and with a tendency to take regular shape (curved edges), the eutectic Mg$_5$ Al$_8$ becomes visible (whitish color that blends with the matrix). Figure 7D shows the Mg$_2$ Si phase with the Al$_6$ (FeMn) phase in the form of ovals at its greatest extent.

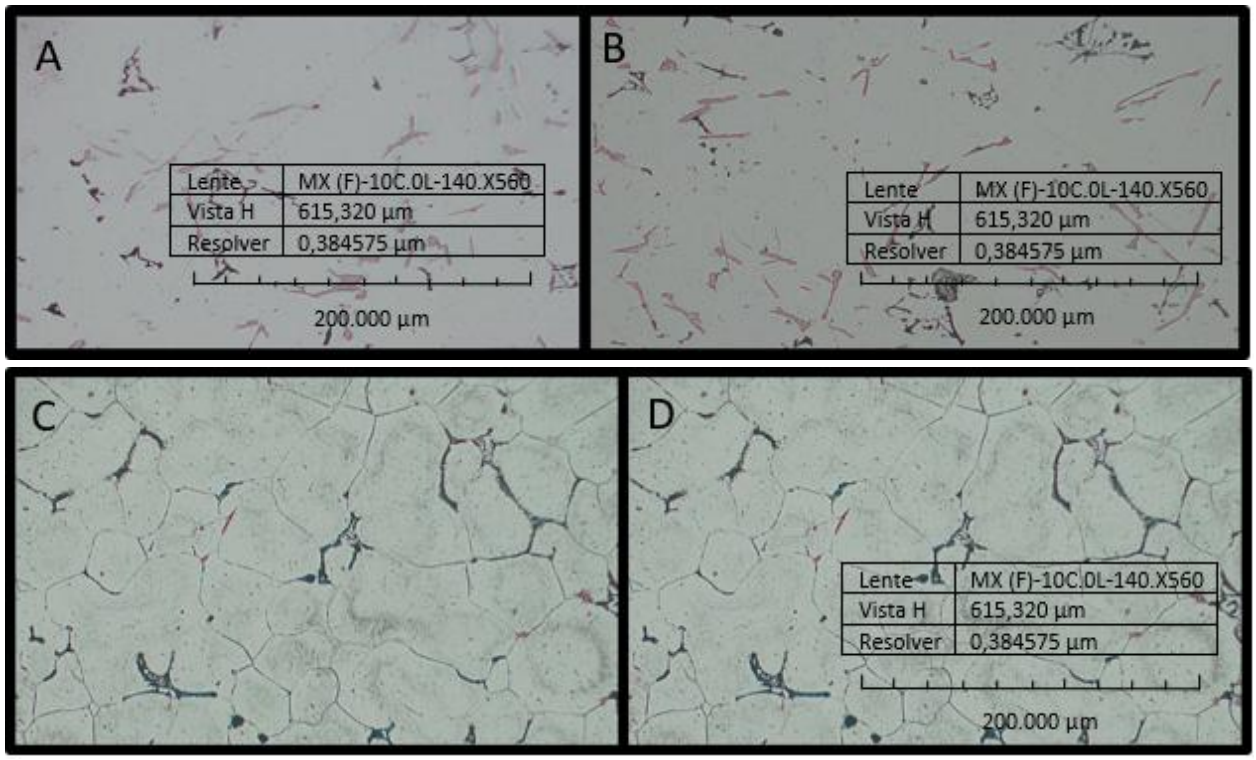

Figure 7. A: Microstructure of alloy T1-B16 560x without etching. B: Microstructure of alloy T2-A10.560x without etching. C: Microstructure of alloy T2-A12.560x 5m (HF) attack. D: Microstructure of alloy T2-A14.560x without attack.

Figure 8A shows the Mg_2 Si phase with the Al_6 (FeMn) phase in needle shapes and the eutectic Mg_5 Al_8 again blending into the matrix as a whole. Figure 8B shows the Mg_2 Si phase tending to take needle shapes, the Al_6 (FeMn) phase has needle and oval shapes. Figure 8C shows the Mg phase$_2$ Si with the Al phase$_6$ (FeMn) which is in greater quantity (compared to the previous figure), and needle and oval shapes. In Figure 8D the Mg2Si phase (Chinese letter) is observed, the Al_6 (FeMn) phase is in needle shapes, the eutectic Mg_5 Al_8 becomes visible.

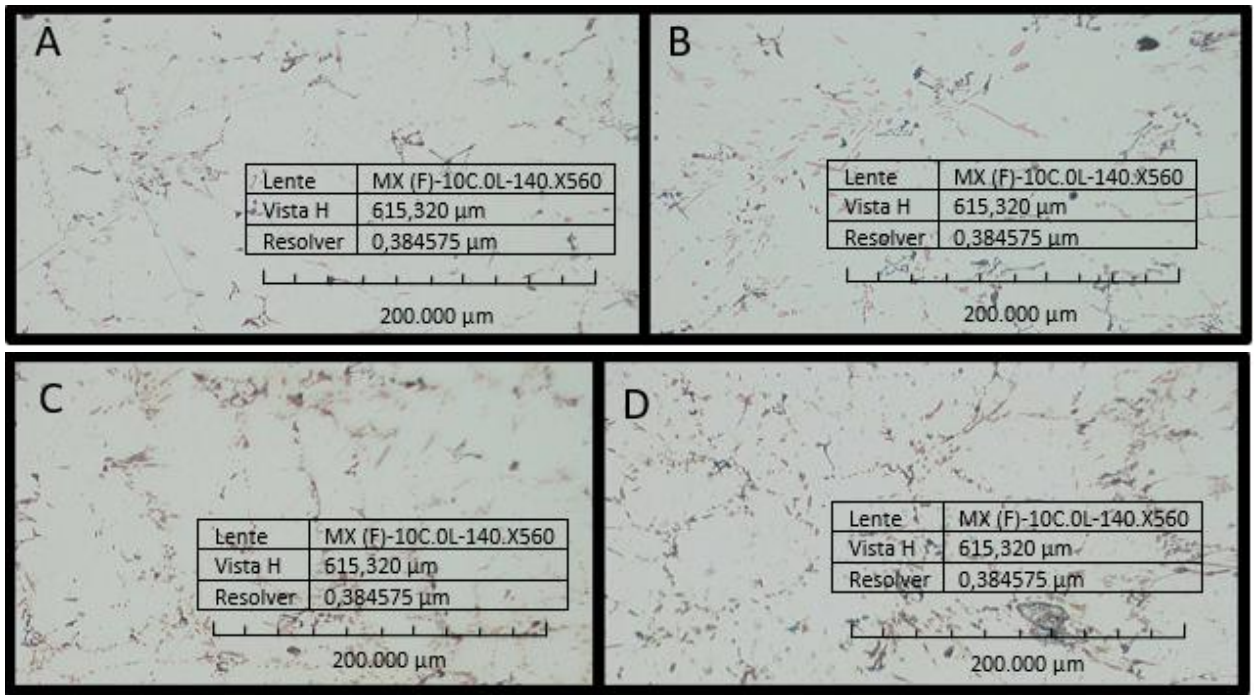

Figure 8. A: Microstructure of alloy T2-A16.560x without etching. B: P14 Microstructure of alloy T2-B10.560x without etching. C: Microstructure of alloy T2-B12.560x without etching. D: Microstructure of alloy T2-B16.560x without etching.

Grain size

The grain size was determined by the intercept method, the results are shown in Table 3. Which shows how the temperature and time of the heat treatment had a great influence on the variation of the grain size and together with this, the concentration of solutes according to each specimen studied gave way to the difference in grain size, among the different alloys.

Table 3. Grain sizes.

Alloy	Average grain diameter (um)	ASTM grain size
Al_5 Mg As cast (A1)	204.9793	1.5
Al_{10} Mg As cast (B1)	223.6102	1.5
Al Mg_{52} Zn As cast (A2)	122.9211	3
Al Mg_{102} Zn As cast (B2)	64.73051	5
T1 - A10	81.19754	4
T1 - A12	74.53814	4.5
T1 - A14	66.24005	5
T1 - A16	49.19502	6
T1 - B10	86.79712	4
T1 - B12	81.89012	4
T1 - B14	58.56062	5.5
T1 - B16	90.06823	4
T2 - A10	100.6849	3.5

T2 - A12	94.60612	3.5
T2 - A14	70.27884	4.5
T2 - A16	89.89745	4
T2 - B10	139.8459	3
T2 - B12	102.4894	3.5
T2 - B14	63.07072	5
T2 - B16	136.6681	3

5. CONCLUSIONS

The study of the influence of cooling rate on 5XXX group alloys, specifically Al_5 Mg and Al_{10} Mg, reveals a complex balance between solidification effects and the resulting mechanical properties. The choice of a die cast, which facilitates rapid cooling, has resulted in a microstructure with a fine grain size and an optimal surface finish. However, this same rapid cooling has led to significant defects such as internal shrinkage, underlining the importance of meticulous control of casting conditions to maximize the quality of the final product. On the other hand, sand castings present additional challenges, such as the formation of porosities caused by the reaction of magnesium with moisture, highlighting the relevance of the casting medium on material integrity. These findings suggest that, although the co-casting technique can result in favorable physical characteristics, it is critical to evaluate and mitigate the adverse effects that rapid cooling rate can have on the structural quality of the alloys.

A first analysis reveals that the methodological design for microstructural etching and revealing was efficient, which allowed the advancement of a detailed further study. Detailed analysis of the microstructures of Al_5 Mg and Al_{10} Mg alloys reveals a significant correlation between the cooling rate and the formation of specific phases. Observations obtained from the analyzed figures show that the morphology of the Mg_2 Si and Al_6 (FeMn) phases varies considerably, suggesting that control of the cooling rate is crucial to optimize the mechanical properties of these alloys. The presence and visibility of the eutectic Mg_5 Al_8 , particularly at grain boundaries, suggests that slow cooling could favor its formation, which could influence the ductility and strength of the alloys. On the other hand, the transition of phase shapes indicates that the solidification and cooling process not only affects the phase distribution, but can also have a profound impact on the final material properties.

The study reveals that both chemical composition and heat treatment parameters, such as temperature and time, are determinants in the grain size of Al_5 Mg and Al_{10} Mg alloys of the 5XXX group. The applied intercept method provides an effective tool to quantify these changes, allowing a better understanding of how solutes and cooling conditions influence the microstructure of the materials.

6. BIBLIOGRAPHIC REFERENCES

[1] B. Davó and J. J. Damborenea, "Corrosion and inhibition in medium-strength aluminum alloys," *Rev. Metal. Vol 40, No 6*, vol. 40, no. 6, pp. 442-446, 2004, doi: 10.3989/revmetalm.2004.v40.i6.304.

[2] R. Falla, K. Quintana, F. Franco, and N. Sanchez, "Mechanical properties of friction stir spot welding in AA6063-T5 aluminum alloy," *Rev. Prospect.*, vol. 10, no. 1, pp. 79-84, 2012, doi:

10.15665/rp.v10i1.399.

[3] J. C. Pereira, L. Durán, D. Deventer, and J. Zambrano, "Torsional mechanical behavior of heat-treated AA6061 aluminum alloy," *Suppl. the Rev. Latinoam. Metal. y Mater.* vol. 28, no. 2, pp. 183-190, 2009.

[4] A. Cotes-Toro, D. Manco-jaraba, and E. Rojas-Martínez, "Evaluation of mechanical and metallurgical properties of Al 5 Mg and Al 10 Mg alloys modified with 2 % Zn after thermal aging treatment," *Prospectiva*, vol. 21, no. 1, pp. 23-31, 2023, doi: 10.15665/rp.v21i1.2948.

[5] Á. Cotes-Toro, D. Manco-Jaraba, and C. Robles-Julio, *Response to thermal aging heat treatment of Al5Mg and Al10Mg alloys modified with 2 % zinc*. Riohacha, Colombia, 2019.

[6] C. Vargel, *The behavior of aluminum and its alloys*, 7th ed. in Encyclopedia of Aluminum. 1981. [Online]. Available: https://books.google.com.co/books?id=nxiktwEACAAJ

[7] K. Van Horn, *Aluminum. Properties, physical metallurgy and phase diagrams*. 1967.

[8] F. De Los Reyes and E. Franco, "Characterization of 12Cr1MoV steel aging from imaging techniques," *Tecnol. Chem*, vol. 29, no. 3, pp. 43-47, 2009.

[9] R. Rodriguez and I. Gutiérrez, "Study of the contribution of phases to mechanical properties in steels with mixed structures," in *VIII Congreso Nacional de Propiedades Mecánicas de Sólidos*, 2002, pp. 87-96.

[10] D. Reigoza, "Microstructural study by optical microscopy with color metallography techniques on an AKT XM 200 motorcycle piston," Universidad Distrital Francisco José de Caldas, 2017.

[11] I. Polmear, D. StJohn, J.-F. Nie, and M. Qian, *Light alloys: metallurgy of the light metals*, 5th ed. Butterworth-Heinemann, 2017.

[12] C. J. Aparicio Bádenas, J. M. Manero Planella, D. Rodríguez Rius, A. Andres Doménech, P. M. Arandés, and J. A. Planell Estany, *Aleaciones ligeras*, 1st ed. Barcelona: Edicions Universitat Politècnica de Catalunya, 2001.

[13] R. M. Nunes *et al.*, *Heat Treating*, 4th ed. 1991.

[14] R. Nunes *et al.*, *ASM Handbook: Properties and Selection: Non Ferreous Alloys and Special-Purporse Materials*, Volume 2. 1990.

[15] ASM Handbook Committee, *Metallography and Microstructures*, 9th ed, vol. 9. USA: Metals Handbook, 1985.

[16] J. E. Hatch, *Aluminum: Properties and Physical Metallurgy*. in Aluminum / J.E. Hatch Hrsg. American Society for Metals. American Society for Metals, 1984. [Online]. Available: https://books.google.com.co/books?id=dUgzGsEMhoUC

[17] L. Mondolfo, *Aluminum Alloys Structure and Properties*, 1st ed. 1976. doi: https://doi.org/10.1016/C2013-0-04239-9.

[18] Foseco, Foundryman's Handbook, 9 edition. England, 1986.

[19] ASTM Standard E3-11, "Metallographic Sample Preparation." ASTM International, pp. 1-7, 2007.

[20] ASTM Standard E - 407, "Standard practice for micro-etching of metals and alloys." ASTM International, 2015. doi: 10.1520 / E0407-07R15E01.

[21] F. Millán-Delgado, "Fabrication and characterization of recycled aluminum alloy with addition of particulate silicon," Universidad Nacional de Colombia, 2016.

[22] G. Dieter, *Mechanical Metallurgy*. McGraw-hill New York, 1961.